

Supporting information for

In Situ and Operando Investigation of the Dynamic Morphological and Phase Changes of
Selenium-doped Germanium Electrode during (De)Lithiation Processes

Tianyi Li^{1‡}, Cheolwoong Lim^{1‡}, Yi Cui¹, Xinwei Zhou^{1,2}, Huixiao Kang¹, Bo Yan^{1,3}, Melissa L. Meyerson⁴, Jason A. Weeks⁴, Qi Liu⁵, Fangmin Guo⁵, Ronghui Kou⁵, Yuzi Liu², Vincent De Andrade⁵, Francesco De Carlo⁵, Yang Ren⁵, Cheng-Jun Sun⁵, C. Buddie Mullins⁴, Lei Chen⁶, Yongzhu Fu⁷, and Likun Zhu^{1*}

¹Department of Mechanical and Energy Engineering, Indiana University Purdue University
Indianapolis, Indianapolis, IN 46202

²Center for Nanoscale Materials, Argonne National Laboratory, 9700 South Cass Avenue,
Argonne, Illinois 60439

³School of Materials Science and Engineering, Shanghai Jiao Tong University, Shanghai,
200030, China

⁴McKetta Department of Chemical Engineering and Department of Chemistry, University
of Texas at Austin, Austin, TX 78712

⁵Advanced Photon Source, Argonne National Laboratory, Argonne, IL 60439

⁶Department of Mechanical Engineering, Mississippi State University, Mississippi State, MS,
39762, USA

⁷College of Chemistry, Zhengzhou University, Zhengzhou 450001, China

‡ These authors contributed equally to this work

*Corresponding author: likzhu@iupui.edu (L. Zhu)

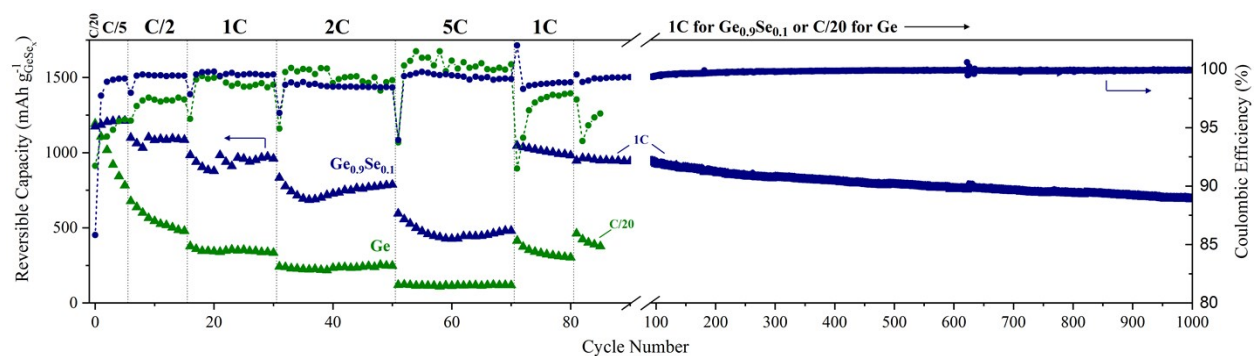


Fig. S1 Galvanostatic discharge cycling of the micro-sized particles of pure Ge-(green data) or $\text{Ge}_{0.9}\text{Se}_{0.1}$ -based (blue data) electrodes showing performance at variable C-rates through 80 cycles following a conditioning cycle at C/20. After 80 cycles, the pure Ge-based electrode was tested at C/20 for five cycles so as to measure the fraction of electrochemically active material remaining: ca. 32%. The $\text{Ge}_{0.9}\text{Se}_{0.1}$ -based electrode was tested at 1 C for 920 additional cycles to assess its long-term stability: the average capacity fade was 0.3 mA h g^{-1} per cycle and the average efficiency was 99.9%.

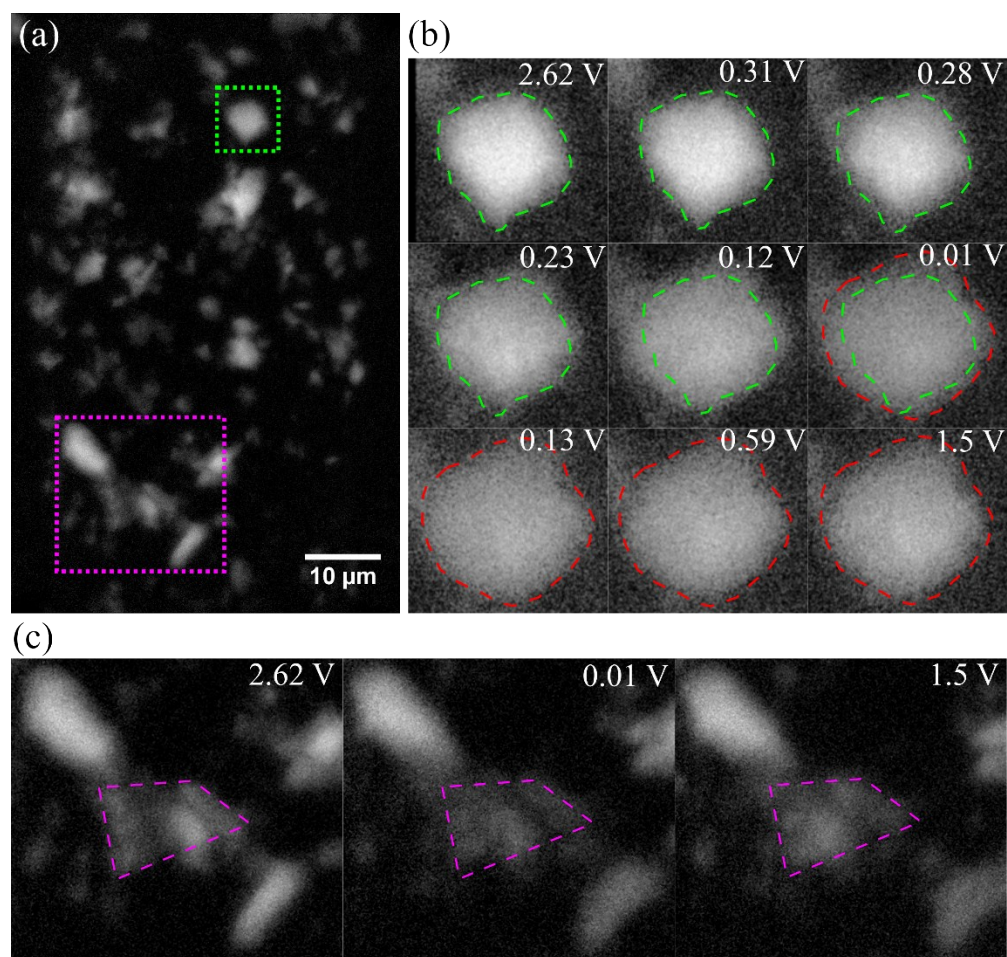


Fig. S2 Operando TXM of Ge electrode. (a) TXM image with 38.8 nm pixel resolution of the pristine Ge electrode for 1 second irradiation at 11.2 keV, (b) TXM dynamic images of a Ge particle (5.3 μm VESD) during the first (de)lithiation under 1 μA, (c) Ge particle cluster changes in pristine (2.62 V), lithiated (0.01 V), and delithiated (1.5 V) states.

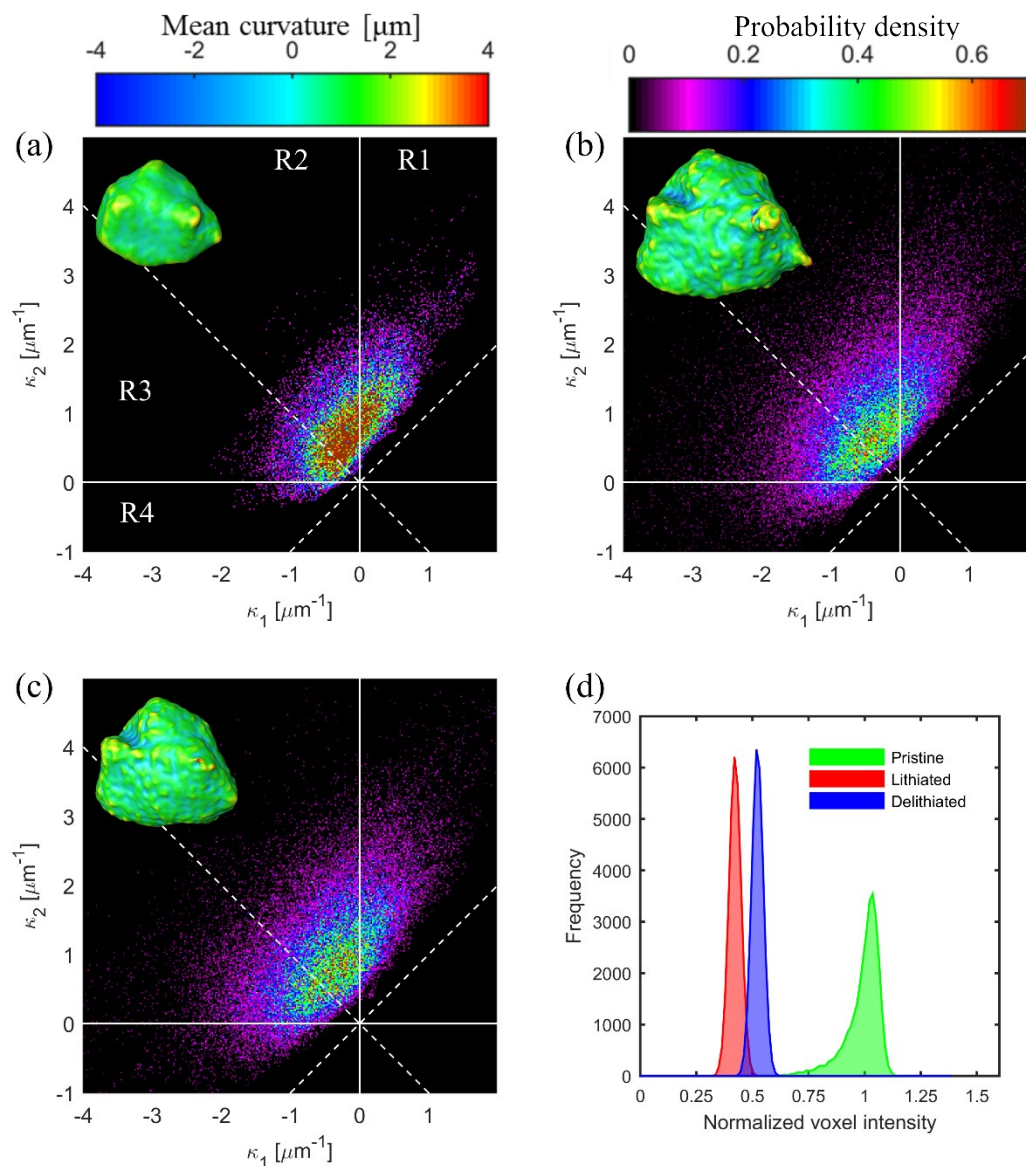


Fig. S3 In situ TXM tomography. Three-dimensional morphologies of the Ge particle shown in Fig. S2b are color mapped with mean curvature on the surfaces of (a) pristine, (b) lithiated, and (c) delithiated conditions. Principal curvatures on the particle surface at different lithiated states are distributed via a distribution known as the Interfacial Shape Distribution (ISD, κ_1 : minimum and κ_2 : maximum principal curvatures). (d) histograms of X-ray attenuation coefficients in the Ge particle. In (a), R1 region indicates convex surface ($\kappa_2 > \kappa_1 > 0$) and R4 region indicates concave surface ($\kappa_1 < \kappa_2 < 0$). Mean curvature is positive in the R1 and R2 regions.

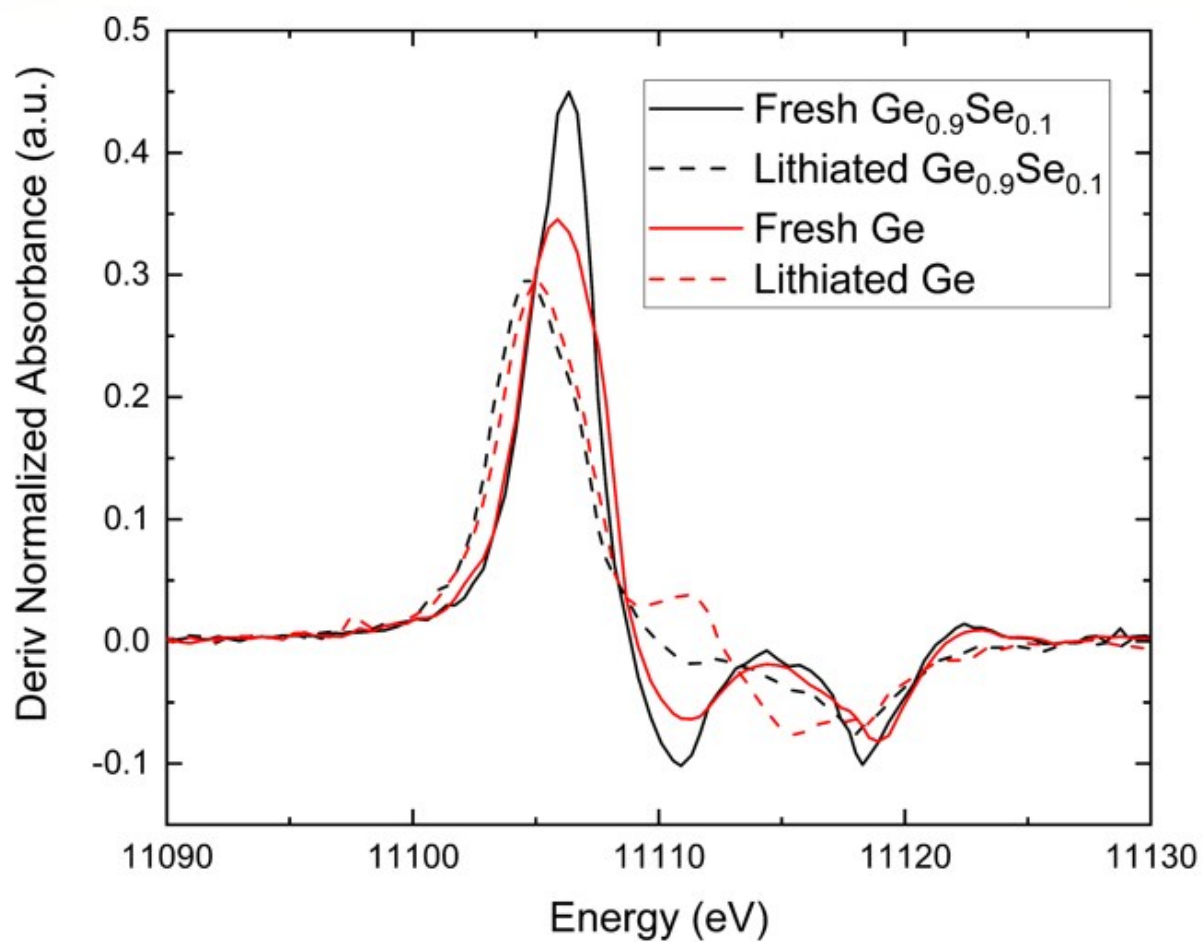


Fig. S4 Normalized first derivatives of XANES spectra in Fig. 4c.

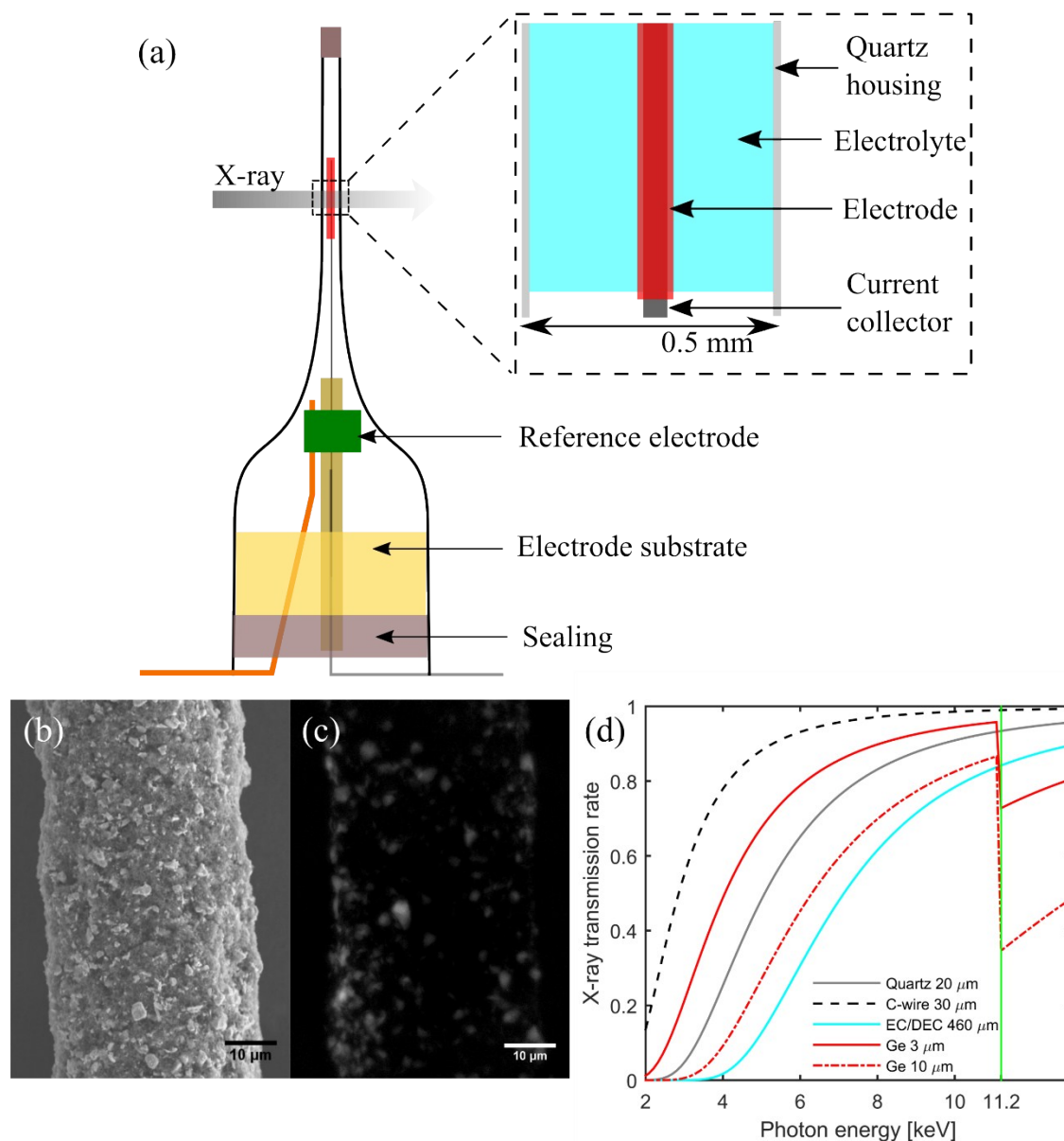


Fig. S5 In situ battery cell. (a) Schematic of the in situ battery cell, (b) SEM image of a pristine Ge electrode on a carbon wire (30 μm) current collector, (c) A TXM image of a pristine Ge electrode in the in situ battery cell, and (d) X-ray transmission rate of the cell components. About 30% of X-ray radiation is absorbed by the quartz capillary, carbon wire, and EC/DEC electrolyte at 11.2 keV.

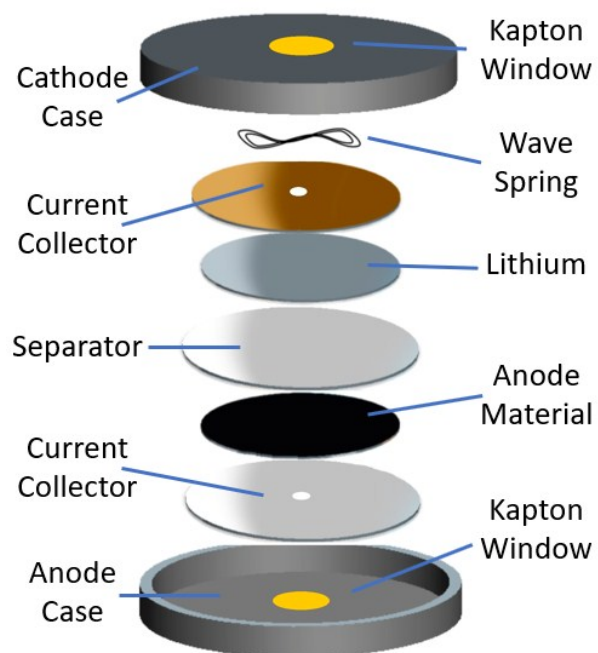


Fig. S6 Schematic of the operando coin cell assembly for operando synchrotron XRD and XAS experiments.

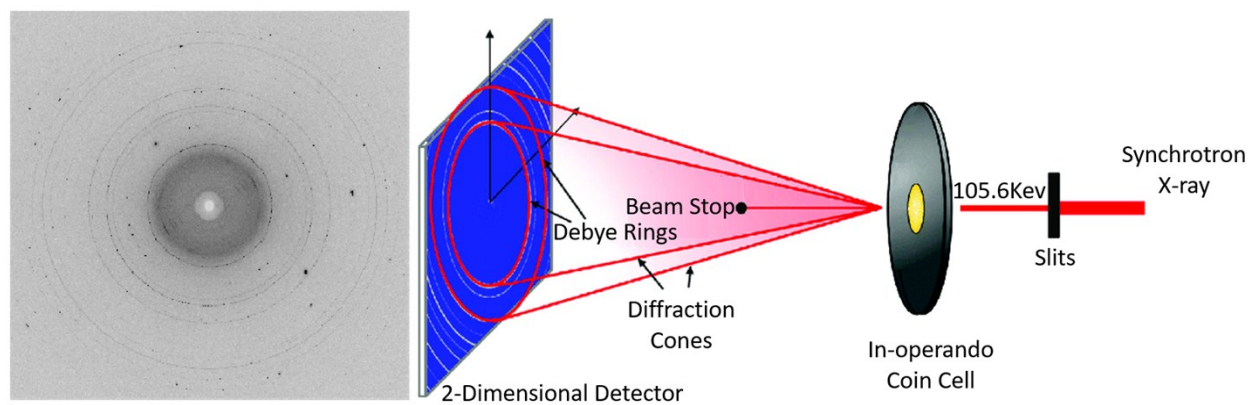


Fig. S7 The synchrotron XRD setup and its resulting diffraction pattern.